Rare Beryllium Icosahedra in the Intermediate Valence Compound CeBe 13 [J. Am. Chem. Soc . 2004 , 126 , 13926−13927].

ARTICLE *in* JOURNAL OF THE AMERICAN CHEMICAL SOCIETY · MAY 2006

Impact Factor: 12.11 · DOI: 10.1021/ja043190c

J|A|C|S
COMMUNICATIONS

Published on Web 10/12/2004

Rare Beryllium Icosahedra in the Intermediate Valence Compound $CeBe_{13}$

Zakiya S. Wilson,[§] Robin T. Macaluso,[§] E. D. Bauer,[†] J. L. Smith,[†] J. D. Thompson,[†] Z. Fisk,[‡] George G. Stanley,[§] and Julia Y. Chan*,[§]

Department of Chemistry, Louisiana State University, Baton Rouge, Louisiana 70803, Materials Science and Technology Division, Los Alamos National Laboratory, Los Alamos, New Mexico 87545, and Department of Physics, University of California, Davis, California 95616

Received July 9, 2004; E-mail: jchan@lsu.edu

It is well-known that α- and *β*-polymorphs of boron and other boron-containing compounds, such as $B_{12}H_{12}^{2-}$ and $B_{12}C_2H_{12}$, adopt 12-membered icosahedral polyhedra.[1−5] Due to the electron deficiency of boron, polyhedral boranes are formed by multicenter 3-center 2-electron bonding, and Wade's rules are often used to explain the bonding in these *closo*-clusters.[6] Be compounds are similarly electron deficient, but polyhedral Be clusters are extremely rare. In $Be_{1.09}B_3$, for example, hexagonal rings occur where each Be atom forms bonds with the two nearest Be neighbors.[7] Linear BeX_2 compounds are commonly formed by the separation of the 2s electron pair into equivalent sp hybrid orbitals. The highest common coordination number of Be found in molecular species is four, with nearly tetrahedral geometries formed via bridging ligands in $BeCl_2$[8] and $[Be(OR)_2]_n$[9] or in discrete complexes such as $[BeF_4]^{2-}$ and $[Be(H_2O)_4]^{2+}$.[10] We report here the first example of a fully characterized beryllium icosahedron in $CeBe_{13}$ that displays intermediate valence behavior. The single-crystal X-ray structure, magnetic susceptibility, and ab initio calculations are reported for this unprecedented Be geometry.

Single crystals of $CeBe_{13}$ were prepared by placing Ce, Be, and Al in the atomic ratio of 1:14:32 into an outgassed BeO crucible and by heating the mixture to 1200 °C under flowing helium. The samples were then cooled for 300 h to the melting point of Al and removed from the furnace. Excess Al was dissolved in NaOH solution, revealing $CeBe_{13}$ single crystals with natural [100] faces.

The structure, shown in Figure 1, was determined by single-crystal X-ray diffraction. Relevant parameters for data collection, refinement, and structure solution are provided as Supporting Information. $CeBe_{13}$ adopts the $NaZn_{13}$ structure type[11] and crystallizes in the cubic space group *Fm*3*c*, $Z = 8$, with the lattice parameter $a = 10.376(2)$ Å. Twelve Be2 atoms form an icosahedron with an isolated Be1 atom located in the center of the polyhedron. The average Be1−Be2 and Be2−Be2 distances are 2.176(2) and 2.270(3) Å, respectively. Each Be_{12} icosahedron of I_h symmetry is surrounded by eight Ce atoms, with the closest Ce−Be2 contact distance of 3.0518(13) Å and Ce−Ce distance of 5.188(1) Å. In turn, each Ce atom is surrounded by 24 Be atoms (8 triangular Be faces from 8 Be_{13} units) in a snub cube environment with O_h site symmetry. The Ce snub cube and the Be_{13} icosahedra adopt a CsCl arrangement. Between the icosahedra are D_{2d} tetracapped tetrahedra, also known as stella quadrangula. The Be2−Be2 bond lengths of 2.267(5)−2.361(5) Å are longer than the 2.106 Å length found in $Be_{1.09}B_3$,[7] but this is consistent with the lower valence electron count and delocalized bonding in this icosahedron.

The electronic structure and bonding in $CeBe_{13}$ was studied via Gaussian 98 using ab initio-restricted Hartree−Fock single-point calculations. A high symmetry $(Be_{13})_8Ce_8(Be_{13})$ cluster model, abstracted from the crystal structure, was used to approximate the solid-state Ce:Be stoichiometry. Calculations were also done on the following model systems: $CeBe_{13}$, Ce_8Be_{13}, $Be_{24}Ce$, and $[Ce_8Be_{13}]^{28+}$ (Supporting Information). The molecular orbital diagrams for Be_{13} and $(Be_{13})_8Ce_8(Be_{13})$ and the selected orbital plots for $(Be_{13})_8Ce_8(Be_{13})$ are shown in Figures 2 and 3.

$CeBe_{13}$ is electron deficient with a valence electron count of only 30, although our $(Be_{13})_8Ce_8(Be_{13})$ model system has one extra Be_{13} cluster present in order to model a high symmetry portion of the solid-state lattice. Because of the few valence electrons available,

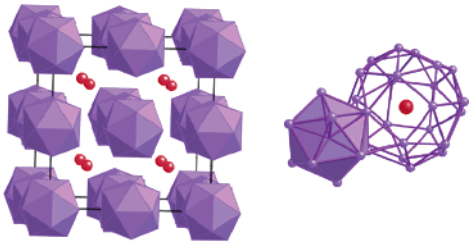

Figure 1. Crystal structure of $CeBe_{13}$ consists of Be_{12} icosahedra (shown by purple shading) in a CsCl arrangement with Ce snub cubes. An isolated Be1 atom is located at the center of the Be_{12} icosahedron, which is composed of Be2 atoms. Red and purple circles represent Ce and Be atoms, respectively.

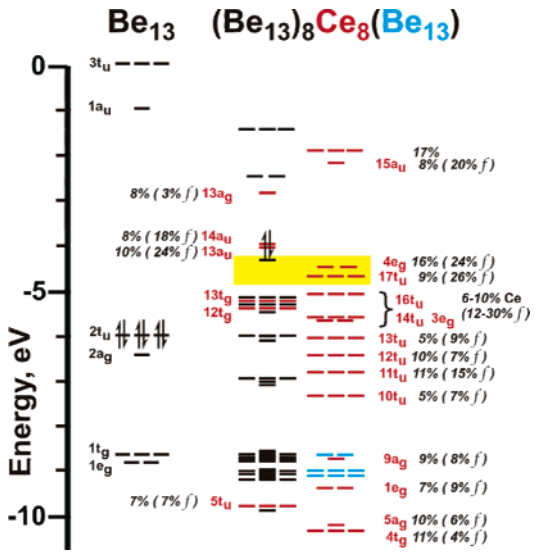

Figure 2. MO diagrams for Be_{13} and $(Be_{13})_8Ce_8(Be_{13})$. The HOMOs are marked by arrows. The MOs in $(Be_{13})_8Ce_8(Be_{13})$ are separated into two columns; the first has mainly outer Be_{13} cluster character, while the second column has significant central Be_{13} character. Red levels have 5% or higher Ce contributions; blue indicates mainly central Be_{13} MOs. The yellow highlighted area indicates the proposed location of the HOMO−LUMO when the extra Be atoms present in the cluster model are taken into account. The percentages are Ce contributions with f orbital compositions.

[§] Louisiana State University.
[†] Los Alamos National Laboratory.
[‡] University of California.

10.1021/ja045861c CCC: $27.50

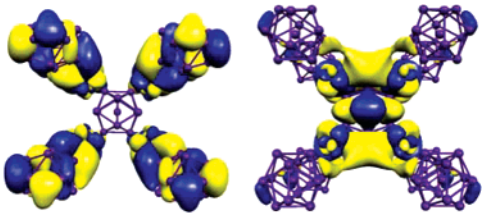

Figure 3. $13a_u$ (left) and $4e_g$ (right) MOs for $(Be_{13})_8Ce_8(Be_{13})$. Purple spheres are Be atoms; red Ce atoms are hidden by orbital lobes.

multicenter bonding is expected and indeed observed. The central Be1 orbital contributions are highly delocalized into the t_u- and a_g-filled levels and represent a minor component in the MOs and will not be discussed further as most of the MO contributions come from the 12 outer Be atoms.

Due to the extra Be_{13} cluster present in the calculation, we believe that the three highest occupied $12-14a_u$ levels should really be empty. The HOMO/Fermi surface would then occur in the vicinity of the $4e_g$ MO, which is 16% Ce and has 24% f character (highlighted region in Figure 2 and MO plot in Figure 3). There is a moderate density of filled and empty MOs in proximity at this energy. The $12-14a_u$ MOs, which are proposed to be part of the conduction band, are only 0.2−0.4 eV higher in energy. The 13 and $14a_u$ MOs also have 18−30% f orbital Ce character (Figure 3). The closeness of these filled and empty orbitals corresponds to a predicted Fermi surface with an overlapping filled−empty band structure for the $CeBe_{13}$ extended solid-state system, consistent with the observed metallic conduction for this material. Many of these MOs provide excellent conductivity pathways through the cluster. The low electron count of the core Be_{13} unit is very important and provides a number of empty MOs that possess Be−Be delocalized bonding character. These can strongly interact with the filled Ce orbitals to generate a 3-D bonding network or band structure.

The $4e_g$ MO, for example, arises from the strong interaction of empty Be sp^3 hybrid orbitals located on a 3-fold vertex of the icosahedron face with Ce dpf hybrid orbitals. There are four-center Be−Be and three-center Ce−Be−Be bonding interactions in this and a number of other lower MOs. This agrees with ELF (electron localization function) calculations, where electron maxima were found at the same locations in ternary trielides with a similar $NaZn_{13}$ structure type.[12]

Although the Ce orbitals are extensively hybridized, almost all of the f character is concentrated in a relatively narrow energy band between −4 and −6 eV, right around the Fermi surface. Previous band structure calculations on $CeBe_{13}$ (using the known $NaZn_{13}$ structure as a template) showed significant f character to the Fermi surface with 46% Ce f band composition.[13]

The calculated average Mulliken charge on the central Be_{13} cluster is −0.39 (+1.3 for the central Be), while the eight outer Be_{13} clusters show larger charge variations of −0.1 to −0.3, with more polarization of the Be atoms that are closer to the Ce centers (+0.69 charge). The low positive charge on the Ce atoms should favor both greater orbital expansion and overlap with the Be clusters, along with enhanced f orbital mixing into the bonding, far more than that in most Ln^{3+} systems. The expansion and greater involvement of f orbital character in M−L bonding could also be significant in low valent solution lanthanide complexes.[14]

In addition to its unusual structural features, $CeBe_{13}$ exhibits intermediate valence behavior, in which valence fluctuations between the Ce $4f^0$ and $4f^1$ states, via hybridization with the conduction electron states, give rise to an enhancement of the effective mass at low temperatures. The hybridization between the localized f electrons and the conduction electrons is responsible

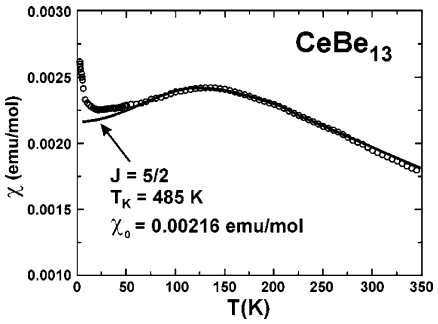

Figure 4. Magnetic susceptibility of $CeBe_{13}$. The large χ and broad maximum at $T_{max} \approx 130$ K is typical of intermediate valence systems.

for the large values of the electronic specific heat coefficient ($\gamma \approx 100$ mJ/mol K^2) and the magnetic susceptibility ($\chi \approx 1 \times 10^{-3}$ emu/mol), which is in marked contrast to those of ordinary metals that have $\gamma \approx 1$ mJ/mol K^2 and $\chi \approx 1 \times 10^{-5}$ emu/mol values. The magnetic susceptibility, $\chi = M/H$ versus T, of a single crystal of $CeBe_{13}$ (Figure 4) exhibits a broad maximum at $T_{max} \approx 130$ K and is typical of intermediate valence systems with an unusually large energy scale (Kondo), $T_K \approx 500$ K. An upturn found below 20 K is likely due to a ferromagnetic impurity phase (since no anomaly is observed in specific heat) and/or a Curie tail contribution from magnetic impurities. If we ignored this upturn below 20 K, the value of the zero-temperature susceptibility is well described by a single impurity Kondo calculation, as shown in Figure 4 using the parameters $T_K = 485$ K and zero-temperature susceptibility $\chi_0 = 2.16 \times 10^{-3}$ emu/mol.[15] The Wilson ratio, $R_W = (\pi^2 \mu_{eff}^2/k_B^2)(\chi_0/\gamma) = 1.01$, which is estimated from the value of χ_0 and $\gamma = 75$ mJ/mol K^2, is close to unity, indicating that the enhancement of both χ and γ at low temperatures is due to itinerant f electrons. The calculated 24% f electron contribution at the Fermi surface is in good agreement with this observation.

Acknowledgment. The authors acknowledge ACS-PRF, NSF CAREER grants (J.Y.C), GIAR from National Academy of Sciences, administered by Sigma Xi (R.T.M), NSF-DMR (Z.F.) for partial support of this work, and NSF (G.G.S). Work at Los Alamos was done under the auspices of the DOE.

Supporting Information Available: Calculational details and additional discussion on all of the models used, along with plots of most of the valence MOs, and crystallographic data. This material is available free of charge via the Internet at http://pubs.acs.org.

References

(1) Koster, R.; Grassberger, M. A. *Angew. Chem., Int. Ed. Engl.* **1967**, *6*, 218.
(2) Lipscomb, W. N. *Boron Hydrides*; Benjamin: New York, 1963.
(3) Muetterties, E. L.; Knoth, W. H. *Polyhedral Boranes*; Dekker: New York, 1969.
(4) Onak, T. *Adv. Organomet. Chem.* **1965**, *3*, 263.
(5) Williams, R. E. *Prog. Boron Chem.* **1970**, *2*, 51.
(6) Wade, K. *Adv. Inorg. Chem. Radiochem.* **1976**, *18*, 1.
(7) Chan, J. Y.; Fronczek, F. R.; Young, D. P.; DiTusa, J. F.; Adams, P. W. *J. Solid State Chem.* **2002**, *163*, 385.
(8) Canadell, E.; Eisenstein, O. *Inorg. Chem.* **1983**, *22*, 3856.
(9) Noth, H.; Schlosser, D. *Inorg. Chem.* **1983**, *22*, 2700.
(10) Cotton, A. F.; Wilkinson, G. *Advanced Inorganic Chemistry*, 5th ed.; John Wiley & Sons: New York, 1988.
(11) Shoemaker, D. P.; Marsh, R. E.; Ewing, F. J.; Pauling, L. *Acta Crystallogr.* **1952**, *5*, 637.
(12) Nordell, K. J.; Miller, G. G. *Inorg. Chem.* **1999**, *38*, 579.
(13) Takegahara, K.; Harima, H.; Kasuya, T. *J. Phys. F: Met. Phys.* **1986**, *16*, 1691.
(14) Evans, W. J.; Lee, D. S.; Ziller, J. W. *J. Am. Chem. Soc.* **2004**, *126*, 454.
(15) Rajan, V. T. *Phys. Rev. Lett.* **1983**, *51*, 308.

JA045861C